Graphical Abstract

To create your abstract, type over the instructions in the template box below.
Fonts or abstract dimensions should not be changed or altered.

Boronic acid inhibitors of the class A β-lactamase KPC-2

Jingyuan Zhou, Paul Stapleton, Shozeb Haider, Jess Healy
UCL School of Pharmacy, 29-39 Brunswick Sq.,

Leave this area blank for abstract info.

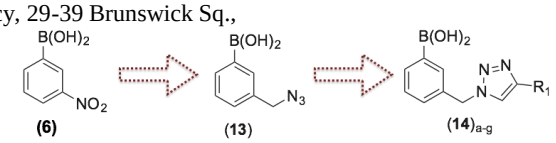

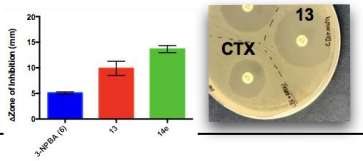

Bioorganic & Medicinal Chemistry
journal homepage: www.elsevier.com

Boronic acid inhibitors of the class A β-lactamase KPC-2

Jingyuan Zhou[a], Paul Stapleton,[a] Shozeb Haider,[a] and Jess Healy[a*]

[a]*UCL School of Pharmacy, 29-39 Brunswick Sq., London, WC1N 1AX, UK*

ARTICLE INFO

Article history:
Received
Received in revised form
Accepted
Available online

Keywords:
KPC
Beta-lactamase
Antibiotic resistance
Boronic acid inhibitors

ABSTRACT

The rapid rise of antimicrobial resistance is one of the greatest challenges currently facing medical science. The most common cause of resistance to β-lactam antibiotics is the expression of β-lactamase enzymes, such as KPC-2. As such the development of novel inhibitors of KPC-2 and related enzymes is of the upmost importance. We report the design and synthesis of novel boronic acids transition state analogs containing a 1,4-substituted 1,2,3-triazole linker based on the known inhibitor 3-nitrophenyl boronic acid and demonstrate that they are promising scaffolds for the development inhibitors of KPC-2 with the ability to recover sensitivity to the antibiotic cefotaxime.

1. Introduction

The rapid rise of antimicrobial resistance is one of greatest challenges currently facing medical science. This coupled with the lack of novel agents reaching the clinic, particularly for the treatment of challenging infections caused by multidrug resistant Gram-negative species, is a cause for serious concern.[1]

One of the most common causes of resistance to β-lactam antibiotics in Gram-negative pathogens is the production of β-lactamase enzymes (BLA's). BLA's have been grouped into 4 classes, A, B, C and D, based on sequence similarity. Class A, C and D are serine BLA's, and the class B enzymes are metallo β-lactamases.[2] KPC is a widespread class A serine β-lactamase with the ability to hydrolyse and neutralize carbapenems, which are considered one of the last lines of defense in tackling challenging infections associated with MDR Gram-negative pathogens. At least 18 variants of this enzyme have been identified, however KPC-2 is the most widespread.[3]

The commonly used β-lactamase inhibitors clavulanic acid (**1**), sulbactam (**2**) and tazobactam (**3**) (Figure 1) are in active against KPC-2, which is particularly challenging to inhibit for a number of reasons; 1) low sequence conservation with other class A enzymes (e.g. 35% SHV-1 and 39% TEM-1) and 2) it has a large and shallow active site allowing it to accommodate bulkier β-lactams. [4-6] In the absence of appropriate and effective β-lactam antibiotic and BLA inhibitor combinations the remaining therapeutic choices are far from ideal (e.g. polymyxins and tigecycline which both have problems associated with toxicity and efficacy).[4] As a result the rapid rise and spread of this enzyme is of serious clinical concern and the development of novel inhibitors is of the upmost importance.

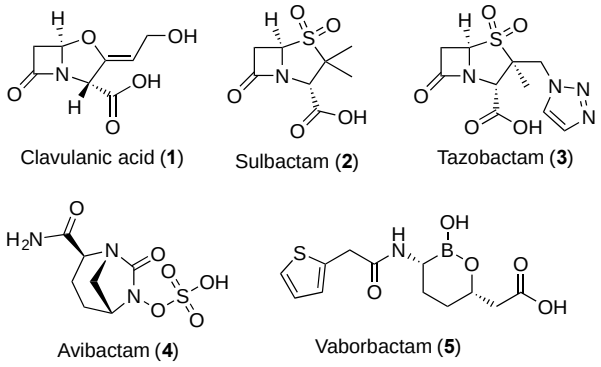

Figure 1. Structures of approved β-lactamase inhibitors.

Despite these problems, a number of BLA inhibitors active against KPC-2 have been reported, including avibactam (Figure 1, **4**), which is a diazocyclooctane, and was approved for use in combination with ceftazidine by the FDA in 2015. Avibactam inhibits many class A and class C BLA's and some class D enzymes but is inactive against the metalloenzymes from class B. However, recent reports of resistance (e.g. Asp179Asn), which emerged within 12 months, are worrying and underline the continued importance of developing novel inhibitors of BLA's.[4,6]

Boronic acids (BA's) were first reported as broad-spectrum inhibitors of BLA's in 1978 by Kiener *et al.*[7] and have been used extensively as tool compounds to study this family of enzymes.[8-10] In recent years they have received renewed interest as transition state (TS) analogs, however, the majority of published studies have focused on AmpC, a class C BLA, as a model system for inhibitor design (**6-11** Figure 2) and compounds exhibit varying

spectra of activities across the different classes of enzymes. [8,11-16] BA's are reversible covalent inhibitors that form a dative bond with the catalytic Ser residue in the enzyme active site (Ser70 in KPC-2). The boron atom in this covalent adduct has a tetrahedral geometry thus mimicking the TS formed during the hydrolysis of β-lactams. As this class of inhibitors is not based on the β-lactam core it is likely to be less sensitive to pre-evolved resistance mechanisms, to mutations and to resistance mechanisms such as BLA upregulation and porin channel deficiencies.[11,13] In 2012 Eidam *et al*. reported the most potent BA inhibitor (**11**) to date with a Ki of 50 pM (AmpC), this dramatic increase in potency relative to previously reported BA's (μM-nM range) was achieved using a combination of structure guided and fragment based drug discovery.[12] The ultimate proof of principle of the utility and importance of the BA class of inhibitors, however, came in 2017 when vaborbactam (Figure 1 (**5**), a cyclic boronic acid) was approved for use by the FDA in combination with meropenem. Vaborbactam (**5**) is a potent inhibitor of class A and C BLA's (including KPC), however, does not inhibit members of the B and D classes. To date no resistance has been reported, however, increased use of this combination will undoubtedly lead to the development of resistance.[6]

Although significant progress has been made, the development of novel inhibitors of KPC-2 (and other challenging BLA's e.g. the class D OXA's which are an emerging clinical challenge and the metallo BLA's for which no inhibitors are available) is still of the upmost importance. Towards this aim, we proposed to develop novel triazole derivatives of the known KPC-2 inhibitor 3-nitrophenyl boronic acid (3-NPBA, **6**). Herein we report the design, synthesis and evaluation of a small library of 1,4-disubstituted 1,2,3-triazole derivatives of 3- or 4-(azidomethyl)phenyl boronic acid scaffolds (**13** & **16**).

2. Materials and Methods

2.1 Chemistry

All materials were purchased from Sigma Aldrich, Fisher and VWR and used without further purification. Anhydrous solvents were purchased from Sigma Aldrich in SureSeal™ bottles. NMR spectra were measured on a Bruker Avance 500 MHz spectrometer and chemical shifts are reported in parts per million (ppm). Mass spectra were measured on Shimadzu LCMS-2020 from solutions of methanol or water, operating in positive or negative mode. HRMS were measured on a Waters QToF Premier from solutions of methanol or water, operating in positive or negative mode.

Preparative and analytical High Performance Liquid Chromatography (HPLC) was performed on an Agilent 1200 Series HPLC system (detection at 254 nm and 220 nm) using reversed phase C18 column (6×50 mm/10×250 mm, 2.5/5 μm (analytical/preparative), XSELECT™ CSH™). Analytical HPLC was conducted using the following conditions: Flow rate: 1.000 mL/min; Gradient conditions: 0-20 min 5-50% B in A, 20-22 min 50-95% B in A; Volume of injection: 10.0 μL. The %purity was calculated by peak area. Preparative HPLC was conducted using the following conditions: Flow rate: 5.000 mL/min; Gradient conditions: 0-49 min 5-40% B in A, 49-50 min 40-70% B in A, 50-52 min 70-95% B in A; Volume of injection: 100.0 μL.

Purification by RP silica gel column chromatography (C18-XS, 15 μm, Interchim) was performed on a Biotage®. Solvent system: 0.1% (v/v) formic acid in water (eluent A) and 0.1% (v/v) formic acid in acetonitrile (eluent B); Flow rate: 5.000 mL/min; Gradient conditions: 0-6 min 100% A, 7-42 min 0-100% B in A, total duration of gradient run was 42 min.

*2.1.1 General procedure for the synthesis of compounds **13 &***

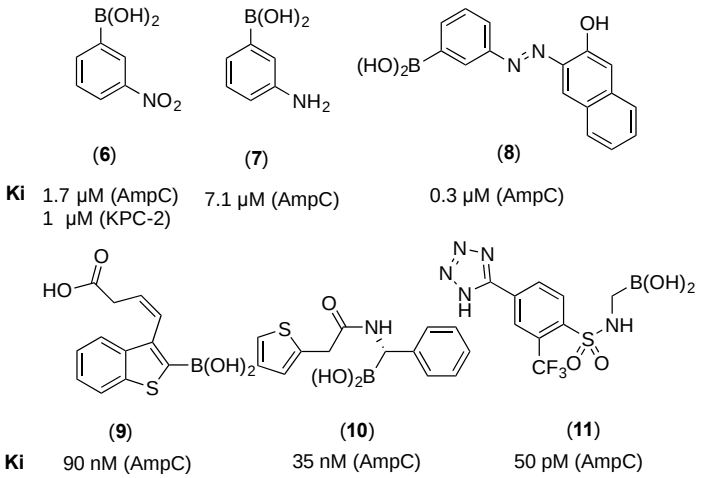

Figure 2. Structures of a selection of published boronic acid transition state analogues.

16

Sodium azide (453 mg, 5 eq) and 3/4-bromomethylphenyl boronic acid (267 mg, 1 eq) were dissolved in anhydrous DMF (5 mL) and stirred at room temperature for 20 hours after which time the reaction was extracted with DCM. The organic layer was washed with brine and dried over anhydrous magnesium sulfate ($MgSO_4$) and concentrated *in vacuo.*

*2.1.1.1 (3-(azidomethyl)phenyl)boronic acid (**13**)*

Pale yellow oil (107 mg, 49%); ^{1}H NMR (500 MHz, CD_3OD) δ 7.75 (s, 1H, ArC<u>H</u>), 7.60-7.55 (m, 1H, ArC<u>H</u>), 7.40-7.37 (m, 2H, ArC<u>H</u>), 4.45 (s, 2H, C<u>H</u>$_2$N$_3$); IR (neat) 3224, 2935, 2862, 2030, 1651, 1608, 1428, 1333, 1170, 787, 701, 644, 574; LC-MS *m/z* 222.2 (M+FA-H$^-$) (RT=2.97, 100%). The data are in agreement with the reported literature values.[17]

*2.1.1.2 (4-(azidomethyl)phenyl)boronic acid (**16**)*

Pale yellow oil (156 mg, 50%); ^{1}H NMR (500 MHz, DMSO-d6) δ 8.10 (s, 2H, B(O<u>H</u>)$_2$), 7.82 (d, *J* = 7.7 Hz, 2H, ArC<u>H</u>), 7.34 (d, *J* = 7.7 Hz, 2H, ArC<u>H</u>), 4.45 (s, 2H, C<u>H</u>$_2$N$_3$); IR (neat) 3042, 2926, 2860, 2102, 1654, 1613, 1341, 1111, 1009, 812, 722, 649, 627; LC-MS *m/z* 222.4 (M+FA-H$^-$) (RT=3.02, 100%). The data are in agreement with the reported literature values.[17]

*2.1.2 General procedure for the synthesis of compounds **14/17a-f***

To a solution of compound **13** or **16** (20 mg, 1 eq) in H_2O:DMF:*t*-BuOH (2.5 mL, 1:3:1), TBTA (0.2 eq), CuBr (0.4 eq) and CsF (2 eq) were added under argon.[18] The required alkyne (1.1 eq) was added dropwise and the reaction stirred for 6 hours at room temperature. After which time 3 mL H_2O:MeOH (1:1) was added and the suspension was filtered under vacuum. The filtrate was further purified by RP column chromatography and preparative HPLC as necessary.

2.1.2.1 (3-((4-(4-methoxyphenyl)-1H-1,2,3-triazol-1-yl)methyl)phenyl)boronic acid (**14a**)

Pale yellow oil (8 mg, 30%); ^{1}H NMR (500 MHz, CD_3OD) δ 8.21 (s, 1H, triazole-C<u>H</u>), 7.80-7.63 (m, 2H, B(OH)$_2$-ArC<u>H</u>), 7.74 (d, *J* = 8.6 Hz, 2H, CH$_3$OArC<u>H</u>), 7.42-7.36 (m, 2H, B(OH)$_2$-ArC<u>H</u>), 6.99 (d, *J* = 8.6 Hz, 2H, CH$_3$OArC<u>H</u>), 5.63 (s, 2H, C<u>H</u>$_2$), 3.83 (s, 3H, OC<u>H</u>$_3$); ^{13}C NMR (125 MHz, CD_3OD) δ 161.4, 138.3, 131.2, 130.1, 129.1, 128.1, 124.2, 121.5 (br, <u>C</u>-B(OH)$_2$), 121.2, 115.4, 115.0, 114.7, 55.8 (O<u>C</u>H$_3$), 55.0 (<u>C</u>H$_2$); IR (neat) 3142,

2947, 2837, 1616, 1499, 1353, 783, 706; LC-MS *m/z* 310.2 ($M+H^+$) (RT=3.34, 100%); HRMS (TOF ES^+) m/z calcd for $C_{16}H_{16}BN_3O_3$ $[M+H]^+$ 310.1366, found 310.1377; HPLC RT 13.14 min, >97% content.

*2.1.2.2 (3-((4-phenyl-1H-1,2,3-triazol-1-yl)methyl)phenyl)boronic acid (**14b**)*

Colourless oil (15 mg, 45%); ^1H NMR (500 MHz, CD_3OD) δ 8.34 (s, 1H, triazole-C<u>H</u>), 7.83 (d, *J* = 7.4 Hz, 2H, ArC<u>H</u>), 7.81-7.64 (m, 1H, $B(OH)_2$-ArC<u>H</u>), 7.63-7.60 (m, 1H, ArC<u>H</u>), 7.43 (d, *J* = 7.4 Hz, 2H, ArC<u>H</u>), 7.45-7.34 (m, 3H, $B(OH)_2$-ArC<u>H</u>), 5.67 (s, 2H, C<u>H</u>$_2$); ^{13}C NMR (125 MHz, CD_3OD) δ 149.3, 142.6, 137.6, 136.0, 134.7, 134.2, 131.6, 130.3 (br, <u>C</u>-$B(OH)_2$), 130.0, 129.5, 128.4, 126.7, 122.3, 55.2 (<u>C</u>H$_2$); IR (neat) 3135, 2943, 2832, 1606, 1430, 1363, 1080, 763, 694; LC-MS *m/z* 279.9 ($M+H^+$) (RT=3.31, 100%); HRMS (TOF ES^+) m/z calcd for $C_{15}H_{14}BN_3O_2$ $[M+H]^+$ 280.1246, found 280.1249; HPLC RT 12.55 min, >98% content.

*2.1.2.3 (3-((4-(pyridin-3-yl)-1H-1,2,3-triazol-1-yl)methyl)phenyl)boronic acid (**14c**)*

Pale yellow oil (5 mg, 21%); ^1H NMR (500 MHz, DMSO-d6) δ 9.06 (s, 1H, pyridine-ArC<u>H</u>), 8.76 (s, 1H, triazole-C<u>H</u>), 8.54 (d, *J* = 3.6 Hz, 1H, pyridine-ArC<u>H</u>), 8.31 (s, 2H, B(O<u>H</u>)$_2$), 8.24-8.21 (d, *J* = 7.9 Hz, 1H, pyridine-ArC<u>H</u>), 7.77-7.76 (m, 2H, $B(OH)_2$-ArC<u>H</u>), 7.48 (dd, *J* = 7.9, 3.6 Hz, 1H, pyridine-ArC<u>H</u>), 7.40-7.37 (m, 2H, $B(OH)_2$-ArC<u>H</u>), 5.67 (s, 2H, C<u>H</u>$_2$); ^{13}C NMR (125 MHz, DMSO-d6) δ 148.9, 146.3, 143.8, 134.7, 133.9, 133.7, 132.4, 129.6, 127.8, 126.6, 124.0, 122.2, 53.4 (<u>C</u>H$_2$), <u>C</u>-$B(OH)_2$ not observed; IR (neat) 3141, 1603, 1423, 1370, 1155, 1052, 783, 709; LC-MS *m/z* 281.0 ($M+H^+$) (RT=2.33, 100%); HRMS (TOF ES^+) m/z calcd for $C_{14}H_{13}BN_4O_2$ $[M+H]^+$ 281.1212, found 281.1230; HPLC RT 4.12 min, >97% content.

*2.1.2.4 (3-((4-(pyridin-2-yl)-1H-1,2,3-triazol-1-yl)methyl)phenyl)boronic acid (**14d**)*

Colourless oil (9 mg, 28%); ^1H NMR (500MHz, CD_3OD) δ 8.47 (s, 1H, ArC<u>H</u>), 8.36-8.08 (m, 1H, pyridine-ArC<u>H</u>), 7.97 (dd, *J* = 7.4, 7.3 Hz, 1H, pyridine-ArC<u>H</u>), 7.87-7.79 (m, 1H, pyridine-ArC<u>H</u>), 7.78-7.71 (m, 1H, $B(OH)_2$-ArC<u>H</u>), 7.67-7.53 (m, 1H, pyridine-ArC<u>H</u>), 7.45 (d, *J* = 7.1 Hz, 1H, $B(OH)_2$-ArC<u>H</u>), 7.41-7.38 (m, 1H, $B(OH)_2$-ArC<u>H</u>), 5.70 (s, 2H, C<u>H</u>$_2$), 4.63 (s, 1H, ArC<u>H</u>); ^{13}C NMR (125 MHz, CD_3OD) δ 165.8, 163.1, 150.3, 138.8, 135.8, 135.6, 135.2, 134.8, 134.4, 131.1 (br, <u>C</u>-$B(OH)_2$), 130.5, 129.4, 124.3, 55.4 (<u>C</u>H$_2$); IR (neat) 3133, 2943, 2832, 1604, 1449, 1115, 1023; LC-MS *m/z* 280.85 ($M+H^+$) (RT=2.55, 100%); HRMS (TOF ES^+) m/z calcd for $C_{14}H_{13}BN_4O_2$ $[M+H]^+$ 281.1212, found 281.1212; HPLC RT 6.83 min, >98% content.

*2.1.2.7 (3-((4-(thiophen-3-yl)-1H-1,2,3-triazol-1-yl)methyl)phenyl)boronic acid (**14e**)*

Colourless oil (18 mg, 34%); ^1H NMR (500MHz, CD_3OD) δ 8.23 (s, 1H, triazole-C<u>H</u>), 7.81-7.64 (m, 2H, $B(OH)_2$-ArC<u>H</u>), 7.64-7.42 (m, 2H, $B(OH)_2$-ArC<u>H</u>), 7.41-7.09 (m, 3H, thiophene-ArC<u>H</u>), 5.64 (s, 2H, C<u>H</u>$_2$); ^{13}C NMR (125 MHz, CD_3OD) δ 144.3, 135.9 (br, <u>C</u>-$B(OH)_2$), 134.7, 134.3, 133.6, 131.0, 130.4, 129.4, 128.7, 126.3, 125.6, 121.6, 55.2 (<u>C</u>H$_2$); IR (neat) 3140, 2932, 1606, 1428, 1338, 1220, 1140, 1050, 794, 755, 704, 588; LC-MS *m/z* 285.9 ($M+H^+$) (RT=3.30, 100%); HRMS (TOF ES^+) m/z calcd for $C_{13}H_{12}BN_3O_2S$ $[M+H]^+$ 286.0824, found 286.0829; HPLC RT 12.10 min, >98% content.

*2.1.2.8 (3-((4-(thiophen-2-yl)-1H-1,2,3-triazol-1-yl)methyl)phenyl)boronic acid (**14f**)*

Colourless oil (36 mg, 67%); ^1H NMR (500MHz, CD_3OD) δ 8.24 (s, 1H, triazole-C<u>H</u>), 7.81-7.63 (m, 2H, $B(OH)_2$-ArC<u>H</u>), 7.76 (s, 1H, thiophene-ArC<u>H</u>); 7.51-7.49 (m, 2H, thiophene-ArC<u>H</u>), 7.48-7.42 (m, 2H, $B(OH)_2$-ArC<u>H</u>), 5.64 (s, 2H, C<u>H</u>$_2$); ^{13}C NMR (125 MHz, CD_3OD) δ 145.5, 136.0 (br, <u>C</u>-$B(OH)_2$), 134.7, 134.2, 132.7, 131.0, 130.3, 129.3, 127.6, 126.7, 122.3, 122.1, 55.2 (<u>C</u>H$_2$); IR (neat) 3131, 2951, 1605, 1429, 1326, 1208, 1142, 1053, 888, 782, 707, 620, 573; LC-MS *m/z* 285.9 ($M+H^+$) (RT=3.26, 100%); HRMS (TOF ES_+) m/z calcd for $C_{13}H_{12}BN_3O_2S$ $[M+H]^+$ 286.0824, found 286.0832; HPLC RT 12.34 min, >98% content.

*2.1.2.5 (4-((4-(4-methoxyphenyl)-1H-1,2,3-triazol-1-yl)methyl)phenyl)boronic acid (**17a**)*

Pale yellow oil (25 mg, 72%); ^1H NMR (500MHz, CD_3OD) δ ^1H NMR (500 MHz, CD_3OD) δ 8.21 (s, 1H, triazole-C<u>H</u>), 7.80-7.65 (m, 2H, $B(OH)_2$-ArC<u>H</u>), 7.73 (d, *J* = 8.8 Hz, 2H, CH_3OArC<u>H</u>), 7.38-7.33 (m, 2H, $B(OH)_2$-ArC<u>H</u>), 6.99 (d, *J* = 8.8 Hz, 2H, CH_3OArC<u>H</u>), 5.65 (s, 2H, C<u>H</u>$_2$), 3.84 (s, 3H, OC<u>H</u>$_3$); ^{13}C NMR (125 MHz, CD_3OD) δ 161.4, 149.2, 135.6, 135.2, 128.2, 128.0, 124.2, 121.5, 115.4, 55.7 (O<u>C</u>H$_3$), 55.0 (<u>C</u>H$_2$), <u>C</u>-$B(OH)_2$ not observed; IR (neat) 3147, 1603, 1571, 1411, 1347, 1051, 1019, 783, 731; LC-MS 310.0 m/z ($M+H^+$) (RT=3.26, 100%); HRMS (TOF ES^+) m/z calcd for $C_{16}H_{16}BN_3O_3$ $[M+H]^+$ 310.1366, found 310.1365; HPLC RT 12.99 min, >99% content.

*2.1.2.5 (4-((4-phenyl-1H-1,2,3-triazol-1-yl)methyl)phenyl)boronic acid (**17b**)*

Colourless solid (18 mg, 54%): ^1H NMR (500MHz, CD_3OD) δ 8.34 (s, 1H, triazole-C<u>H</u>), 7.83 (d, *J* = 7.4 Hz, 2H, ArC<u>H</u>), 7.81-7.65 (m, 2H, $B(OH)_2$-ArC<u>H</u>), 7.44 (dd, *J* = 7.4, 7.3 Hz, 2H, ArC<u>H</u>), 7.40-7.34 (m, 3H, $B(OH)_2$-ArC<u>H</u> & ArC<u>H</u>), 5.67 (s, 2H, C<u>H</u>$_2$); ^{13}C NMR (125 MHz, CD_3OD) δ 149.2, 135.6, 135.2, 131.6, 130.0, 129.4, 128.2, 126.7, 122.3, 55.0 (<u>C</u>H$_2$), <u>C</u>-$B(OH)_2$ not observed; IR (neat) 3160, 1615, 1411, 1344, 765, 694; LC-MS *m/z* 279.9 ($M+H^+$) (RT=3.27, 100%); HRMS (TOF ES^+) m/z calcd for $C_{15}H_{14}BN_3O_2$ $[M+H]^+$ 280.1260, found 280.1266; HPLC RT 12.68 min, >99% content.

*2.1.2.6 (4-((4-(pyridin-3-yl)-1H-1,2,3-triazol-1-yl)methyl)phenyl)boronic acid (**17c**)*

Pale yellow oil (11 mg, 33%); ^1H NMR (500MHz, CD_3OD) δ 9.03 (s, 1H, triazole-C<u>H</u>), 8.57-8.44 (m, 2H, pyridine-C<u>H</u>), 8.29 (d, *J* = 8.2 Hz, 1H, pyridine-ArC<u>H</u>), 7.67-7.52 (m, 2H, $B(OH)_2$-ArC<u>H</u>), 7.53 (dd, *J* = 8.2, 4.9 Hz, 1H, pyridine-ArC<u>H</u>), 7.43-7.26 (m, 2H, $B(OH)_2$-ArC<u>H</u>), 5.70 (s, 2H, C<u>H</u>$_2$); ^{13}C NMR (125 MHz, CD_3OD) δ 149.6, 147.2, 145.8, 135.3, 135.0, 128.7, 128.3, 125.7, 123.2, 122.8, 116.8, 55.1 (<u>C</u>H$_2$), <u>C</u>-$B(OH)_2$ not observed; IR (neat) 3131, 1612, 1411, 1345, 1050, 805, 704; LC-MS *m/z* 281.0 ($M+H^+$) (RT=2.04, 100%); HRMS (TOF ES^+) m/z calcd for $C_{14}H_{13}BN_4O_2$ $[M+H]^+$ 281.1212, found 281.1221; HPLC RT 3.69 min, >97% content.

*2.1.2.6 (4-((4-(pyridin-2-yl)-1H-1,2,3-triazol-1-yl)methyl)phenyl)boronic acid (**17d**)*

Pale yellow oil (16 mg, 51%); ^1H NMR (500MHz, CD_3OD) δ 8.70-8.50 (m, 1H, pyridine-ArC<u>H</u>), 8.43 (s, 1H, triazole-C<u>H</u>), 8.17-8.02 (m, 1H, pyridine-ArC<u>H</u>), 7.93 (t, *J* = 7.5 Hz, 1H, pyridine-ArC<u>H</u>), 7.79-7.66 (m, 2H, $B(OH)_2$-ArC<u>H</u>), 7.44-7.32 (m, 3H, $B(OH)_2$-ArC<u>H</u> & pyridine-ArC<u>H</u>), 5.71 (s, 2H, C<u>H</u>$_2$); ^{13}C NMR (125 MHz, CD_3OD) δ 151.0, 150.4, 148.9, 138.9, 138.4,

137.8, 135.6, 135.3, 128.4, 124.7, 124.2, 121.7, 55.1 ($\underline{C}H_2$), $\underline{C}$-$B(OH)_2$ not observed; IR (neat) 3147, 1603, 1571, 1411, 1347, 1051, 1019, 783, 731; LC-MS *m/z* 280.9 ($M+H^+$) (RT=2.47, 100%); HRMS (TOF ES^+) m/z calcd for $C_{14}H_{13}BN_4O_2$ $[M+H]^+$ 281.1212, found 281.1215; HPLC RT 5.51 min, >97% content.

2.1.2.9 (4-((4-(thiophen-3-yl)-1H-1,2,3-triazol-1-yl)methyl)phenyl)boronic acid ***(17e)***

Colourless oil (11 mg, 23%); ^1H NMR (500MHz, CD_3OD) δ 8.23 (s, 1H, triazole-C$\underline{H}$), 7.80-7.65 (m, 2H, $B(OH)_2$-ArC$\underline{H}$), 7.42-7.40 (m, 2H, thiophene-ArC$\underline{H}$), 7.37-7.34 (m, 2H, $B(OH)_2$-ArC$\underline{H}$), 7.10-7.09 (m, 1H, thiophene-ArC$\underline{H}$), 5.64 (s, 2H, C$\underline{H}_2$); ^{13}C NMR (125 MHz, CD_3OD) δ 144.3, 135.6, 135.3, 133.6, 128.7, 128.3, 128.1, 126.4, 125.6, 121.7, 55.0 ($\underline{C}H_2$); IR (neat) 3124, 3095, 2832, 1613, 1415, 1342, 1165, 1047, 717; LC-MS *m/z* 285.9 ($M+H^+$) (RT=3.23, 100%); HRMS (TOF ES^+) m/z calcd for $C_{13}H_{12}BN_3O_2S$ $[M+H]^+$ 286.0824, found 286.0826; HPLC RT 11.92 min, >99% content.

2.1.2.10 (4-((4-(thiophen-2-yl)-1H-1,2,3-triazol-1-yl)methyl)phenyl)boronic acid ***(17f)***

Pale yellow oil (19 mg, 40%); ^1H NMR (500MHz, CD_3OD) δ 8.23 (s, 1H, triazole-C$\underline{H}$), 7.80 (d, *J* = 7.1 Hz, 1H, $B(OH)_2$-ArC$\underline{H}$), 7.76-7.74 (m, 1H, thiophene-ArC$\underline{H}$), 7.66 (d, *J* = 7.4 Hz, 1H, $B(OH)_2$-ArC$\underline{H}$), 7.51-7.48 (m, 2H, thiophene-ArC$\underline{H}$), 7.37 (d, *J* = 7.4 Hz, 1H, $B(OH)_2$-ArC$\underline{H}$), 7.32 (d, *J* = 7.1 Hz, 1H, $B(OH)_2$-ArC$\underline{H}$), 5.64 (s, 2H, C$\underline{H}_2$); ^{13}C NMR (125 MHz, CD_3OD) δ 144.7, 134.8, 134.4, 131.9, 127.4, 127.3, 126.8, 125.9, 121.5, 121.3, 54.2 ($\underline{C}H_2$); IR (neat) 3124, 3095, 2832, 1612, 1413, 1345, 1082, 1050, 781, 715; LC-MS *m/z* 286.0 ($M+H^+$) (RT=3.19, 100%); HRMS (TOF ES^+) m/z calcd for $C_{13}H_{12}BN_3O_2S$ $[M+H]^+$ 286.0824, found 286.0828; HPLC RT 11.71 min, >96% content.

2.1.3 Synthesis of *(3-((4-benzyl-1H-1,2,3-triazol-1-yl)methyl)phenyl)boronic acid* ***(14g)***

To a solution of compound **13** (30 mg, 1 eq) in H_2O:DMF:*t*-BuOH (2.5 mL, 1:3:1), TBTA (36 mg, 0.4 eq), CuBr (20 mg, 0.8 eq) and CsF (103 mg, 4 eq) were added under argon. 3-phenyl-1-propyne (0.02 mL, 1.1 eq) was added dropwise. The reaction was stirred for 4-6 hours at 35 ºC, after which time 3 mL H_2O:MeOH (1:1) was added. The suspension was filtered under vacuum and the filtrate further purified by RP column chromatography and preparative HPLC to afford colourless oil (4 mg, 10%); ^1H NMR (500MHz, DMSO-d6) δ 8.37-8.26 (br d, *J* = 12.9 Hz, 2H, B(O$\underline{H}$)$_2$), 8.22 (d, *J* = 7.2 Hz, 1H, $B(OH)_2$-ArC$\underline{H}$), 7.87-7.69 (m, 3H, $B(OH)_2$-ArCH & Bn-ArC$\underline{H}$), 7.59 (t, *J* = 7.8, 7.2 Hz, 2H, $B(OH)_2$-ArC$\underline{H}$), 7.45-7.37 (m, 1H, Bn-ArC$\underline{H}$), 7.33-7.19 (m, 3H, Bn-ArC$\underline{H}$), 5.71 (s, 2H, C$\underline{H}_2$), 5.52 (s, 2H, C$\underline{H}_2$), 3.98 (s, 1H, triazole-C$\underline{H}$); ^{13}C NMR (125 MHz, DMSO-d6) δ 146.3, 139.6, 135.0, 134.3, 134.0 (br, $\underline{C}$-$B(OH)_2$), 133.2, 129.9, 128.5, 128.4, 127.7, 126.1, 122.5, 53.3 ($\underline{C}H_2$), 52.9 ($\underline{C}H_2$); IR (neat) 3152, 2943, 2821, 1591, 1449, 1353, 1115, 1023, 803, 707; LC-MS *m/z* 294.0 ($M+H^+$) (RT=3.44, 100%); HRMS (TOF ES^+) m/z calcd for $C_{16}H_{16}BN_3O_2$ $[M+H]^+$ 294.1417, found 294.1419; HPLC RT 6.83 min, >98% content.

2.2 Disk diffusion assay

Disk diffusion assays were carried out using the *Escherichia coli* strain BL21(DE3) transformed with pET30a KPC-2C plasmid (obtained from Focco Van den Akker). The protocol was based on the Clinical and Laboratory Standards Institute System (CLSI) guidelines where S(susceptible), I(intermediate) and R(resistant) are defined as zones of inhibition surrounding the disk of <22, 23-25 and >26 mm respectively.[19] The assay was performed on Meuller Hinton (MH) agar plates containing 200 µM IPTG, and plated with a suspension of cells in MH broth made up to a 0.5 McFarland standard equivalent. The sterile blank and cefotaxime (30 µg) disks were obtained from Oxoid supplied by Thermo Scientific™. Boronic acid inhibitors were dissolved in DMSO (5 mg/mL), 10 µL of which were applied onto the required disks, giving a final concentration of 50 µg/disk. The agar plates were incubated at 37 °C overnight and the diameter of the zone of inhibition for each disk measured in mm. The change in diameter was calculated relative to the CTX-DMSO control.[20]

2.3 In silico docking

The crystal structure of KPC-2 β-lactamase in complex with boronic acid transition state analog 3-NPBA (PDB id 3RXX)[20] was used as a starting point to study binding of boronic acid analogs to KPC-2.[21] The chemical structures of the ligands were sketched, built and docked using ICM-Pro software (www.molsoft.com). The charges were computed and assigned using the ICFF force field.[22] The spatial position of the existing 3-NPBA ligand in the crystal structure was used to define the binding region of ligands. The grid maps were constructed around this region and extended at least 7Å beyond every atom of 3-NPBA. Docking was performed using the automated covalent docking module in the ICM-Pro software. Ser70 was selected as the residue to be modified with a covalent bond on reaction with the ligands. The serine β-lactamase covalent mechanism was selected as the reaction and docking was run employing a thoroughness of 5.0 and generating five docked conformations for each ligand. The final docked conformation was chosen based on the strongest binding energy between the docked ligand and the KPC-2 receptor. All figures were generated using the ICM-Pro software.

2.3 MIC determination

Microorganisms: *Escherichia coli* NCTC10118 is a susceptibility testing control strain, *E. coli* BL21 (DE3) was transformed with a plasmid encoding an inducible KPC-2 β-lactamase (class A β-lactamase), *E. coli* G69 expresses the plasmid-mediated class C β-lactamase CMY-4, *Klebsiella pneumoniae* NCTC13443 produces the class B metallo-β-lactamase NDM-1 and *K. pneumoniae* expresses a CTX-M-type β-lactamase (class A β-lactamase). *E. coli* NCTC10118 and *E. coli* NCTC13443 were obtained from the National Collection of Typed Cultures (London, UK). *E. coli* G69 and *K. pneumoniae* 342 are clinical isolates held in the culture collection of P. Stapleton (UCL School of Pharmacy). For KPC expressing strain BL21 (DE3) transformed with pET30a KPC-2C was used as before.

The MIC of cefotaxime in the presence and absence of the β-lactamase inhibitors were determined by a microdilution technique in a 96-well microplates in Isosensitest Broth (Oxoid, UK). Cefotaxime was evaluated over a concentration range of 32 to 0.03 µg/mL and inhibitor compounds were tested at a fixed concentration of 50 µg/mL. An inoculum of 0.5×10^5 colony forming units (CFU) of organism per mL and a total volume of 100 µL was used. *E. coli* BL21 (DE3) expressing an inducible KPC-2 β-lactamase plasmid was evaluated in the presence of 1 mM IPTG to ensure enzyme production. Results were determined by visual inspection after incubation at 37 °C for 16 hours. The MIC is defined as the lowest concentration of the antimicrobial agent that inhibits visible growth of the organism. In all cases the concentration ranges were two-fold serial dilutions and the quantity of the solvent dimethyl sulfoxide (DMSO) present did not exceed 1% (a level known not to affect bacterial growth; unpublished observation).

3.0 Results and Discussion

3.1 Ligand design

A significant number of studies have been reported in which simple phenylboronic acid scaffolds have been employed in the development of inhibitors of serine BLA's from class A, C and to a lesser extent D with substituents in both the 3- and 4-position relative to the boronic acid moiety (some examples shown in Figure 2). Building on this prior knowledge we proposed to employ the reported inhibitor 3-NPBA (**6**),[20] for which an X-ray crystal structure bound to KPC-2 has been published, as a scaffold to design a series of novel triazole analogues to explore the SAR of KPC-2. 3-NPBA provides a good starting point for medicinal chemistry optimization; it is small and fragment-like

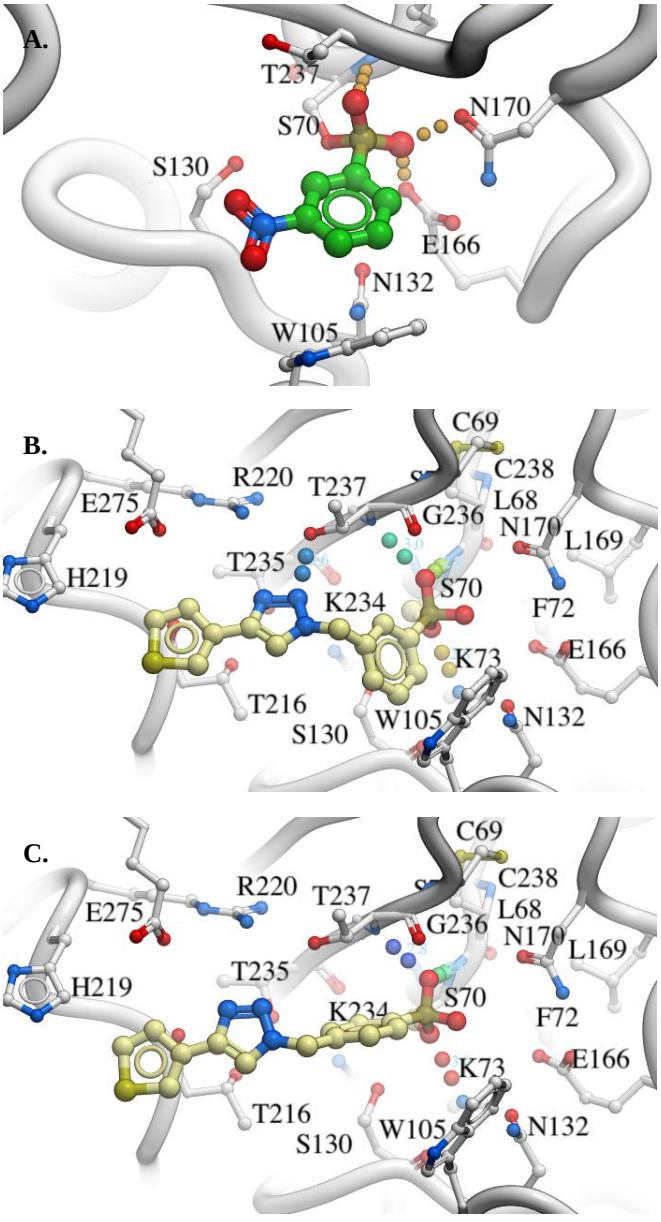

Figure 3. A. X-ray crystal structure of 3-NPBA (pdb code: 3RRX) **B.** Docking of compound **14e** (docking score: -26.12) **C.** Docking of compound **17e** (docking score: -24.36). Polar contacts represented by dotted lines.

with a K_i in the low micromolar range and it forms an extensive network of interactions with the enzyme active site (Figure 3 A). The B-OH groups are positioned in the oxyanion hole and the deacylation water pockets respectively and form polar contacts with N170 and E166. In addition the phenyl ring forms an edge to face π-stacking interaction with W105 and π-cation interactions with K73 and N132. The NO_2 at the 3-position, however, is far

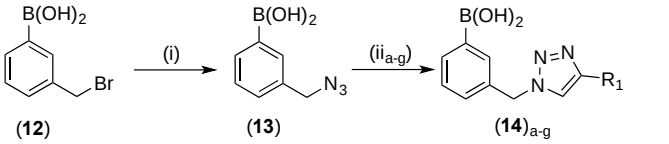

(**a**) R_1 = (4-OCH_3)Ph, (**b**) R_1 = Ph
(**c**) R_1 = 3-Pyr, (**d**) R_1 = 2-Pyr
(**e**) R_1 = 3-thiophene, (**f**) R_1 = 2-thiophene,
*(**g**) Bn

Scheme 1. Synthesis of *para* triazole analogues. *Reagents and conditions:* (i) 3-Bromomethylphenyl boronic acid (1 eq), NaN_3 (5 eq), DMF, RT, 20 h, 49% (ii) **13**, alkyne (1.1 eq), TBTA (0.2 eq), CuBr (0.4 eq), CsF (2 eq), H_2O:DMF:*t*-BuOH (1:3:1), RT, 6 h, (a) 30%, (b) 45%, (c) 21%, (d) 28%, (e) 34%, (f) 67%, (g) 10%. *for 3-phenyl-1-propyne increased eq of TBTA, CuBr and CsF were added and the reaction was heated to 35 °C for 4-6 h.

from optimal, forming no polar contacts with the enzyme active site and there is an appropriate vector and available space to build off this position and to develop novel inhibitors with improved affinity.

Towards this aim we designed a series of 3- and 4-position analogs employing click chemistry to incorporate a 1,2,3-triazole linker. These scaffolds allow exploration of the most appropriate reaction vector for derivatisation and examination of the SAR of the system. Triazoles are appealing linkers for a number of reasons, the chemistry is robust and flexible, the triazole has a dipole moment equivalent to an amide bond and is capable of forming hydrogen-bonding interactions.[23] Covalent docking of a series of 1,4-disubstituted 1,2,3-triazoles with aromatic substituents, both 5 and 6 membered rings and H-bond acceptors and donors, was performed in which the boron atom formed a covalent bond with the active site serine residue. Extensive exploration of properties and position of substituents on the aromatic ring has not been explored but will be addressed in future work. Key interactions observed in the published X-ray crystal structure of 3-NPBA and KPC-2 were recapitulated in the docked structures (e.g. H-bonds with Thr237 and K73) (representative examples shown Figure 3 B & C). A methylene unit was incorporated between the phenyl boronic acid ring the azide moiety to increase flexibility. The triazole linker is predicted to form a hydrogen bond with the hydroxyl group of Thr237 in the *meta* analogs and the aromatic substituent predicted to pack against a relatively hydrophobic α-helix in both the *meta* and *para* analogs. Due to the small size of the library all compounds were selected for synthesis and biological evaluation.

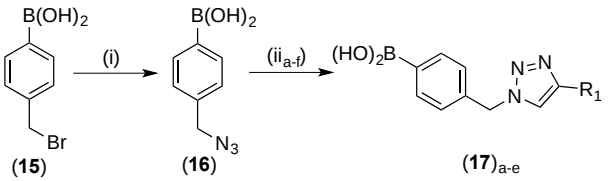

(**a**) R_1 = (4-OCH_3)Ph, (**b**) R_1 = Ph
(**c**) R_1 = 3-Pyr, (**d**) R_1 = 2-Pyr
(**e**) R_1 = 3-thiophene, (**f**) R_1 = 2-thiophene

Scheme 2. Synthesis of *para* triazole analogues. *Reagents and conditions:* (i) (i) 4-Bromomethylphenyl boronic acid (1 eq), NaN_3 (5 eq), DMF, RT, 20 h, 50% (ii) **16**, alkyne (1.1 eq), TBTA (0.2 eq), CuBr (0.4 eq), CsF (2 eq), H_2O:DMF:*t*-BuOH (1:3:1), RT, 6 h, (a) 72%, (b) 54%, (c) 33%, (d) 51%, (e) 23%, (f) 40%.

3.2 Synthesis of 1,4-substituted triazole analogues

Towards the synthesis of the selected analogs the required azido derivatives **13** and **16** were synthesized by S_N2 substitution of the required bromomethyl compounds (**12** & **15**). This furnished the azide scaffolds in moderate yield (49 and 50% respectively, Scheme 1 & 2 (i)).

With the azide scaffolds in hand we next set about making the 1,4 triazole analogs using standard copper catalysed click chemistry. This proved unsuccessful in our hands and a review of the literature, however, revealed that the addition of fluoride, in the form of CsF, was required to protect the boronic acid moiety and prevent/minimize copper insertion into the C-B bond and the associated decomposition reactions.[18] As a result the conditions employed for the Huisgen 1,3-dipolar cycloaddition reaction were as follows; TBTA (0.2 eq), CuBr (0.4 eq) and CsF (2 eq) in H_2O:DMF:t-BuOH (1:3:1). This allowed the synthesis of the desired triazole analogues in moderate yield (23-72%).

The unconjugated benzyl alkyne derivatives (e.g. **14g**) proved less reactive and required more forcing conditions, TBTA (0.4 eq), CuBr (0.8 eq) and CsF (4 eq) in H_2O:DMF:t-BuOH (1:3:1) and heating to 35 °C. This difference in reactivity may be attributed to the higher pKa of the terminal alkyne *c.f.* the conjugated alkynes (acetylide formation is a rate determining step in CuAAC).[24] Despite these changes, the reaction was sluggish and afforded the triazole **14g** in low yield (10%). For the *para* analogue an insufficient quantity of pure material was obtained to proceed with characterization and susceptibility testing. More forcing conditions will be explored in the future.

3.3 Susceptibility testing

With the triazole analogs in hand we first set about assessing their ability to recover the sensitivity of an *E. coli* strain (BL21 DE3) containing an inducible KPC-2 plasmid to cefotaxime (CTX) using the disk diffusion assay.[20] All compounds were tested at a concentration of 50 µg/disk + 30 µg of the antibiotic CTX. The MH agar contained 200 µM IPTG to ensure sufficient expression of KPC-2 to result in a resistant phenotype. In all

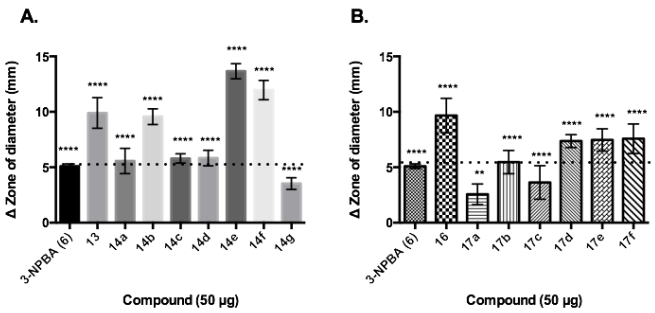

Figure 4. Susceptibility testing; disk diffusion assay. **A.** Bar graph of the change in zone of clearance relative to control (CTX + DMSO) for 3-position analogues. **B.** Bar graph of the change in zone of clearance relative to control (CTX + DMSO) for 3-position analogues. Statistical significance was evaluated relative to CTX+DMSO using a one way ANOVA. **** $p < 0.0001$, *** $p < 0.001$, ** $p < 0.01$, * $p < 0.05$.

cases, with the exception of **14g**, **17a**, and **17c**, the diameter of the zone of inhibition increased sufficiently to alter the phenotype from resistant to susceptible (Figure 4 **A** & **B**) indicating the promise of these novel triazole derivatives for medicinal chemistry optimisation. The triazoles were also tested in the absence of CTX and no zone of inhibition was observed in all cases, suggesting that the inhibitors do not have bactericidal activity in their own right and that the observed effect is a result of inhibition of KPC-2 (data not shown).

Looking at the data in more detail, it appears that the relatively conservative change from a nitro group to a methyl azido group is tolerated in both cases (i.e. *meta* (**13)** and para (**16**), Figure 4 A & B) with a greater zone of inhibition observed relative to the positive control 3-NPBA. For the *meta* analogues **14a**, **14c**, **14d**, and **14g**, no statistically significant change was observed relative to 3-NPBA, however, a decrease in the zone of clearance was observed relative to the starting azido scaffold (**13**), suggesting that the triazole analogs are not optimal. The phenyl substituted triazole (**14b**) exerted a similar effect to the un-derivatised azido scaffold. For the thiophene analogues, **14e** and **14f**, however a statistically significant increase in the zone of inhibition was observed relative to both 3-NPBA and **13** suggesting that smaller substituents at the 4 position of the triazole are better tolerated than phenyl or benzyl rings. Analysis of the docking predictions reveals that this may be the result of improved packing of the thiophene analogs against the hydrophobic loop between α10 and α11 helices (Figure 5A). The design and synthesis of further analogs is required to validate this observation. For the *para* analogues, **17b** and **17c** exerted a similar effect to 3-NPBA and treatment with **17a** resulted in a smaller zone of inhibition *c.f.* 3-NPBA. In all cases, **17a-c**, the triazole was less favourable than

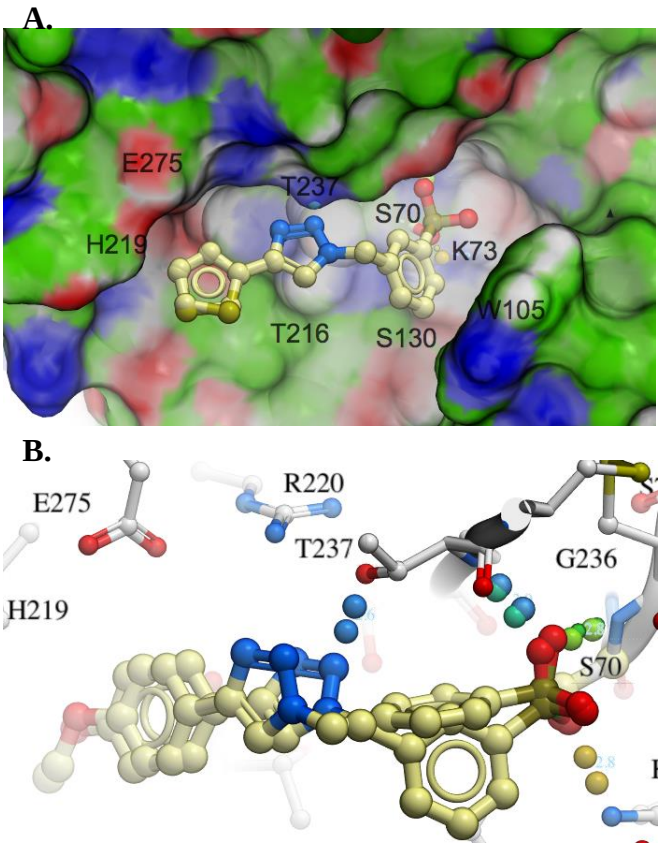

Figure 5. A. Docking of **14e** and **14f** with surface charges. **B.** Overlay of docking of **14a** and **17a**. Polar contacts represented by dotted lines.

the unsubstituted azido scaffold (**16**). No improvement relative to the azido scaffold was observed for compounds **17d-f**. Looking at the docking in more detail suggests that the key difference between the *meta* and *para* analogs is the formation of a key hydrogen bond between the triazole linker and Thr237. In the *para* analogues the phenyl ring is twisted, resulting a 1.65Å displacement of the triazole from Thr237, thus preventing the formation of this key interaction (Figure 5 B). The disk diffusion

data correlates well with the *in silico* predications and provides further insight into the observed SAR. Future studies will employ X-ray crystallography and enzyme kinetics to examine the above SAR in more detail and to guide the design of second-generation analogs.

To provide further insight into the spectrum of activity of the boronic acid inhibitors described above MIC's were determined with CTX against a range of clinical strains expressing class A, B, C and D BLA's (Table 1 and TableS1). No KPC producing clinical isolate was available and so the strain containing the KPC-2 plasmid employed for the disk diffusion experiments was employed to determine the MIC in this case. Treatment of BL21 (DE3) pET30a KPC2C with 50 μg/mL of all BA compounds synthesized resulted in renewed sensitivity to CTX. The MIC decreased from 16 μg/mL to ≤ 0.03 μg/mL (533 fold increase in susceptibility to CTX) in all cases with the exception of **14a**, **17a** and **17f** for which the MIC decreased to 0.12, 0.06 and 0.12 μg/mL respectively (133-266 fold increase in susceptibility to CTX). The compounds were inactive against all other strains tested, with the exception of **13** and 3-NPBA which resulted in a small decrease in MIC for CTX in *E. coli* G69 (CMY-4), which produces a class C AmpC like β-lactamase suggesting that these may yet provide good scaffolds for the development of inhibitors with a broader spectrum of activity. To elucidate any trends future work will re-evaluate the compounds at lower concentrations and test against a panel of more clinically relevant KPC producing strains.

3. Conclusions

We have demonstrated that analogs of the known inhibitor 3-NPBA containing a 1,4-disubstituted 1,2,3-triazole are promising scaffolds for the development of potent inhibitors of the class A BLA KPC-2. Susceptibility testing and *in silico* docking revealed that the *meta* analogs perform better than the corresponding *para* analogs. It is proposed that the key difference between the regioisomers is the ability of the triazole ring to form a H-bond with residue Thr326 which is absent in the *para* analogs. The results discussed above also suggest that smaller substituents at the 4-position of the triazole ring are better tolerated, most likely due to improved packing against the hydrophobic loop between α10 and α11 helices. Future work will explore this hypothesis *via* the design, synthesis and evaluation of a second generation of triazole analogs with more varied substituents at the 4-position. Furthermore to explore both the SAR and spectrum of activity in more detail IC_{50}'s of the compounds described above will be determined against a panel of BLA's, in addition to evaluation against a more clinically relevant KPC producing strain.

Table 1. MICs for cefotaxime in the presence of 50 μg/mL boronic acid inhibitors

Inhibitor	*E. coli* NCTC10118	*E. coli* BL21DE3 (KPC-2)**	*E. coli* G69 (CMY-4)$^{\Delta}$
CTX*	≤0.03	16	>32
14a	≤0.03	0.12	32
14b	≤0.03	≤0.03	>32
14c	≤0.03	≤0.03	>32
14d	≤0.03	≤0.03	>32
14e	≤0.03	≤0.03	>32
14f[#]	≤0.03	≤0.03	>32
17a	≤0.03	0.06	>32
17b	≤0.03	≤0.03	>32
17c	≤0.03	≤0.03	>32
17d	≤0.03	≤0.03	>32
17e	≤0.03	≤0.03	>32
17f	≤0.03	0.12	>32
13	≤0.03	≤0.03	8
16	≤0.03	≤0.03	>32
3NPBA	≤0.03	≤0.03	8

* CTX, cefotaxime MIC in absence of inhibitor.
** KPC-2 expression induced with 1 mM IPTG.
# compound **14g** was not tested.
Δ Data for *K. pneumoniae* NCTC13443 (NDM-1) and *K. pneumoniae* 342 (CTX-M-type) not shown all MIC >32 μg/mL.

References and notes

(1) Richard J Fair, Y. T. *Perspectives in Medicinal Chemistry* **2014**, *6*, 25–64.

(2) Ambler, R. P. *Phil. Trans. R. Soc. Lond. B* **1980**, *289*, 321–331.

(3) Stoesser, N.; Sheppard, A. E.; Peirano, G.; Anson, L. W.; Pankhurst, L.; Sebra, R.; Phan, H. T. T.; Kasarskis, A.; Mathers, A. J.; Peto, T. E. A.; Bradford, P.; Motyl, M. R.; Walker, A. S.; Crook, D. W.; Pitout, J. D. *Sci. Rep.* **2017**, *7*, 5917–254ra126.

(4) Barnes, M. D.; Winkler, M. L.; Taracila, M. A.; Page, M. G.; Desarbre, E.; Kreiswirth, B. N.; Shields, R. K.; Nguyen, M.-H.; Clancy, C.; Spellberg, B.; Papp-Wallace, K. M.; Bonomo, R. A. *mBio* **2017**, *8*, e00528–17.

(5) Papp-Wallace, K. M.; Bethel, C. R.; Distler, A. M.; Kasuboski, C.; Taracila, M.; Bonomo, R. A. *Antimicrob. Agents Chemother.* **2010**, *54*, 890–897.

(6) Bush, K. *ACS Infect. Dis.* **2017**, doi; acsinfecdis.7b00243.

(7) Kiener, P. A.; Waley, S. G. *Biochem. J.* **1978**, *169*, 197–204.

(8) Beesley, T.; Gascoyne, N.; Knott-Hunziker, V; Petursson, S.; Waley, S. G.; Jaurin, B.; Grundström, T. *Biochem. J.* **1983**, *209*, 229–233.

(9) Pasteran, F.; Mendez, T.; Guerriero, L.; Rapoport, M.; Corso, A. *J. Clin. Microbiol.* **2009**, *47*, 1631–1639.

(10) Pournaras, S.; Poulou, A.; Tsakris, A. *J. Antimicrob. Chemother.* **2010**, *65*, 1319–1321.

(11) Eidam, O.; Romagnoli, C.; Caselli, E.; Babaoglu, K.; Pohlhaus, D. T.; Karpiak, J.; Bonnet, R.; Shoichet, B. K.; Prati, F. *J. Med. Chem.* **2010**, *53*, 7852–7863.

(12) Eidam, O.; Romagnoli, C.; Dalmasso, G.; Barelier, S.; Caselli, E.; Bonnet, R.; Shoichet, B. K.; Prati, F. *Proc. Natil. Acad. Sci.* **2012**, *109*, 17448–17453.

(13) Drawz, S. M.; Bonomo, R. A. *Clin. Microbiol. Rev.* **2010**, *23*, 160–201.

(14) Buzzoni, V.; Blázquez, J.; Ferrari, S.; Calò, S.; Venturelli, A.; Costi, M. P. *Bioorg. Med. Chem. Lett.* **2004**, *14*, 3979–3983.

(15) Tondi, D.; Calò, S.; Shoichet, B. K.; Costi, M. P. *Bioorg. Med. Chem. Lett.* **2010**, *20*, 3416–3419.

(16) Tondi, D.; Powers, R. A.; Caselli, E.; Negri, M.-C.; Blázquez, J.; Costi, M. P.; Shoichet, B. K. *Chem. Biol.* **2001**, *8*, 593–611.

(17) Fedorov, A. Y.; Shchepalov, A. A.; Bol shakov, A. V.; Shavyrin, A. S.; Kurskii, Y. A.; Finet, J. P.; Zelentsov,

S. V. *Russian Chemical Bulletin 53*, 370–375.
(18) Jin, S.; Choudhary, G.; Cheng, Y.; Dai, C.; Li, M.; Wang, B. *Chem. Commun.* **2009**, 5251–5253.
(19) Coyle, M. B. *Manual of antimicrobial susceptibility testing*; asm.org, 2005.
(20) Ke, W.; Bethel, C. R.; Papp-Wallace, K. M.; Pagadala, S. R. R.; Nottingham, M.; Fernandez, D.; Buynak, J. D.; Bonomo, R. A.; van den Akker, F. *Antimicrob. Agents Chemother.* **2012**, *56*, 2713–2718.
(21) Nguyen, N. Q.; Krishnan, N. P.; Rojas, L. J.; Prati, F.; Caselli, E.; Romagnoli, C.; Bonomo, R. A.; van den Akker, F. *Antimicrob. Agents Chemother.* **2016**, *60*, 1760–1766.
(22) Katritch, V.; Totrov, M.; Abagyan, R. *J Comput Chem* **2003**, *24*, 254–265.
(23) Bonandi, E.; Christodoulou, M. S.; Fumagalli, G.; Perdicchia, D.; Rastelli, G.; Passarella, D. *Drug Discovery Today* **2017**, *22*, 1572–1581.
(24) Zhang, X.; Liu, P.; Zhu, L. *Molecules* **2016**, *21*, 1697.

Supplementary Material

Supplementary material available as pdf. .

Acknowledgments

The authors would like to acknowledge Weixian Mao and Anna Stankiewicz for their help with this project.